The role of chloride transport in the control of the membrane potential in skeletal muscle — Theory and experiment

Jill Gallaher [a], Martin Bier [a,*], Jan Siegenbeek van Heukelom [b]

[a] Dept. of Physics, East Carolina University, Greenville, NC 27858, USA
[b] Swammerdam Institute for Life Sciences, Center for Neurosciences, University of Amsterdam, Amsterdam, The Netherlands

ARTICLE INFO

ABSTRACT

We present a model for the control of the transmembrane potential of mammalian skeletal muscle cell. The model involves active and passive transport of Na^+, K^+, and Cl^-. As we check the model against experimental measurements on murine skeletal muscle cells, we find that the model can account for the observed bistability of the transmembrane potential at low extracellular potassium concentration. The effect of bumetanide, a blocker of the Na,K,2Cl-cotransporter, is measured and modeled. A hyperosmotic medium is known to stimulate the Na,K,2Cl-cotransporter and we also measure and model the effects of such a medium. Increased chloride transport has two effects on the interval along the extracellular potassium concentration axis where the system is bistable: the interval is shifted towards higher potassium concentrations and the length of the interval is reduced. Finally, we also obtain estimates for the chloride permeability ($P_{Cl} = 2 \times 10^{-5}$ cm/s), for the transmembrane chemical potential of chloride, and for the steady state flux through the Na,K,2Cl-cotransporter (2×10^{-11} mol/cm^2 s for chloride).

1. Introduction

The maintenance of an electrochemical gradient across the membrane is essential for a living cell to stay alive [1]. For a mammalian skeletal muscle cell, the inside is about −75 mV relative to the outside. There are, furthermore, significant differences in intra- and extracellular concentrations for the most prominent ions. For sodium we have $[Na^+]_i \approx 10$ mM versus $[Na^+]_o \approx 150$ mM, for potassium $[K^+]_i \approx 130$ mM versus $[K^+]_o \approx 5.7$ mM, and for chloride $[Cl^-]_i \approx 8$ mM versus $[Cl^-]_i \approx 120$ mM. The electrochemical gradients are primarily maintained by Na,K-ATPase, also called the Na,K-pump [2]. This pump hydrolyzes ATP and utilizes the released energy from one ATP to move three Na^+ ions, against a strong electrochemical potential, from the inside to the outside of the cell. In the course of the same cycle two K^+ ions are moved into the cell.

Both the chemical and the electric gradient drive Na^+ to the inside of the cell. However, Na^+ channels in the membrane are mostly closed. At steady state the low sodium permeability and the high electrochemical potential for sodium lead to a sodium inflow that equals the Na,K-pump driven outflow. For K^+ the electric and the chemical force have opposite directions and almost balance each other out. Under normal conditions a significant fraction of the K^+ channels is open and the ensuing potassium permeability is high. This sets up a force towards a steady state in which the transmembrane electric

potential, V_m, is close to a value where it compensates for the K^+ chemical transmembrane potential. The chemical transmembrane potential for K^+ is $E_K = (RT/F)\log([K^+]_o/[K^+]_i)$. Here, and throughout this article, the symbol "log" denotes the natural logarithm. In mammalian muscle cells a large part of the potassium permeability is due to the so-called inwardly rectifying potassium channels (IRK). These channels protect the high intracellular potassium concentration through a rectification property: they are mostly open when $V_m \lesssim E_K$ (i.e. when the net force drives K^+ into the cell) and mostly closed when $V_m \gtrsim E_K$ (i.e. when the net force drives K^+ out of the cell). In normal physiological steady state conditions $V_m − E_K$ is slightly above zero. This leads to a steady leak of potassium ions out of the cell. A variety of IRK channels exists and especially those in cardiac cells are extensively studied [3].

In this article we go beyond just the Na^+ and K^+ transport, and we include Cl^- ions into the picture. Chloride is an important ion in the regulation of the transmembrane potential and there is growing research interest in the different channels, transporters and pumps that are involved in its transport. The membrane's permeability for chloride has been reported to be up to about an order of magnitude higher than the permeability for potassium [4]. So, just like for K^+, for Cl^- the electric potential and the chemical potential almost balance each other out. What keeps $[Cl^-]_i$ slightly above equilibrium with respect to $[Cl^-]_o$ is the activity of the Na,K,2Cl-cotransporter. The Na,K,2Cl-cotransporter imports 2 Cl^- ions in conjunction with one K^+ ion and one Na^+ ion. The electrochemical gradient for Na^+ provides the energy to import the other three ions. The Na,K,2Cl-cotransporter thus

* Corresponding author.
 E-mail address: bierm@ecu.edu (M. Bier).

couples the transmembrane electrochemical potential of Cl$^-$ to the transmembrane electrochemical potentials of Na$^+$ and K$^+$.

The Na,K,2Cl-cotransporter only imports ions into the cell and because of this it plays a central role in a cell's osmotic regulation and volume homeostasis [5–7]. As such, the cotransporter is also important in the function of the kidney. Bumetanide blocks the Na,K,2Cl-cotransporter very effectively (it is known as a "high ceiling loop diuretic") and it is frequently administered to patients with excessive accumulation of body fluids, hypertension, and congestive heart failure [8].

In this article we present a mathematical model for the steady state electrochemical balance of a cell. We test the model against electrophysiological measurements on impaled muscle cells. In both the model and in the experiment we follow how the electric transmembrane potential at steady state changes as the extracellular potassium concentration, $[K^+]_o$, is decreased to values that are significantly below the physiological level and next increased again back to the physiological level. We then stop the pumping of chloride through the application of bumetanide. After such application the chloride distribution will simply follow the electric potential, i.e. $E_{Cl} = V_m$, and chloride concentrations will no longer affect the steady state membrane potential. We examine the low $[K^+]_o$ regime with and without bumetanide on the same cell and we compare model predictions with the actual experiment. A hyperosmotic medium is a medium in which the osmotic value is elevated through the addition of molecules that can't permeate the cell membrane. Such a medium is known to stimulate the Na,K,2Cl-cotransporter [5–7]. So hyperosmolarity has the opposite effect of bumetanide. We also examine the low $[K^+]_o$ regime for one and the same cell with and without such medium hyperosmolarity. Subsequently, we again compare model predictions with experimental outcomes.

Our study of the control of the transmembrane potential at low extracellular $[K^+]$ bears significance for the understanding of hypokalemia. This is a disorder in which the K$^+$ concentration in the blood becomes low (<3.5 mM). The ailment often arises acutely in connection with diuretic therapy or renal malfunction [9,10]. Hypokalemia can also occur as a periodically returning symptom in certain inherited disorders [11,12]. Clinical manifestations of hypokalemia can consist of decreased muscle function and even paralysis. Electrophysiological experiments and models show that, at a sufficiently low extracellular potassium, a second steady state emerges [13,14]. The membrane potential in this steady state is about −50 mV. It has been suggested that the observed paralysis comes about as a result of cells switching to this depolarized state [15].

Intuitively it can be understood that at a hypophysiological $[K^+]_o$, a hyperpolarization is necessary for the transmembrane chemical force on K$^+$ and the transmembrane electrical force on K$^+$ to keep canceling each other out. The driving force for potassium ions increases as the hyperpolarization of E_K is larger than the hyperpolarization of V_m. A hyperpolarized V_m also leads to increased leak of Na$^+$ and the hyperpolarized steady state thus requires more "pump work" on the part of the Na,K-ATPase. However, there is a critical point in the dynamics. The pump has a saturation level and there is a critical value of $[K^+]_o$ below which the increased leak of Na$^+$ into the cell at the more negative membrane potential can no longer be compensated for by pumping activity. A hyperpolarized steady state is then no longer tenable. The increased Na,K-pump activity has also increased the intracellular potassium concentration and thereby $(V_m - E_K)$. When $(V_m - E_K)$ crosses a threshold, the IRKs close and a "switch" to the depolarized state takes place. In the depolarized state V_m is about 60% of what is was in the hyperpolarized steady state. The about tenfold reduced potassium permeability accounts for a steady state in which the high intracellular potassium concentration is "protected" even though there is a large outward directed driving force, $(V_m - E_K)$, for potassium ions. In [14] a simpler model was presented that involved only sodium and potassium. That model employed a Michaelis–Menten description for the behavior of the Na,K-ATPase and used simple conductance characteristics for Na$^+$-channels and for K$^+$-channels (including the IRKs). The eventual dynamical system indeed exhibited a switch from a hyperpolarized state to a depolarized state at low $[K^+]_o$. The analysis of the model, furthermore, revealed a parameter range where both the hyperpolarized state and the depolarized state constitute stable solutions. Such bistability is also experimentally observed with murine skeletal muscle cells [13,17–20]. In this article we present a more complete electrochemical model by also bringing chloride into the picture.

When we employ a constant P_K that is about two orders of magnitude larger than the P_{Na}, the bistability is no longer there. This is seen in actual experiments [15] as well as upon analysis of the ensuing dynamical system. So the rectification properties of the IRKs are essential for the bistable dynamics. In a future publication we will elaborate on this.

Near physiological conditions it is the small P_{Na} that determines V_m. The membrane potential, after all, has to be brought to a level that is sufficiently negative to get the passive inward flow that steady state requires. P_K and P_{Cl} are very high and, at any electric membrane potential, E_K and E_{Cl} will be very close to V_m. The cotransporter flow is driven by the sodium electrochemical potential and, for its effect on the membrane potential, the cotransporter acts as an addition to the sodium permeability. So, blocking the cotransporter works out electrochemically like decreasing the P_{Na}. Such blocking therefore leads to a hyperpolarization. Stimulation of the Na,K,2Cl-cotransporter with hyperosmolarity leads, in turn, to a small depolarization.

Ref. [16] speculates on the possibility of constructing a numerical model to make some of the above arguments more solid and quantitative. Below we present such a model and report on the results of simulation. We survey the bistability region of one and the same cell with and without bumetanide. We also survey the bistability region of one and the same cell with an iso-osmotic extracellular medium and a hyperosmotic extracellular medium. We adjust model settings to fit the experiments and this allows us to estimate important parameters of pumps and channels. We also quantitatively assess the role of Cl$^-$ in the maintenance of the membrane potential.

2. The model

Fig. 1 specifies the components that are going into our model. Below we will spell out how the flow through each of these components depends on concentrations, on the membrane potential and on other constant parameters.

In our model the source of the transmembrane potential is the Na, K-ATPase. This pump moves 2 K$^+$ ions and 3 Na$^+$ ions at every cycle [2]. We thus assume second and third order Michaelis–Menten kinetics for the transmembrane flux:

$$J_P\left(\left[\mathrm{Na}^+\right]_i\right) = \alpha_X J_P^{Max}\left(1 + \frac{K_m^K}{[K^+]_o}\right)^{-2}\left(1 + \frac{K_m^{Na}}{[Na^+]_i}\right)^{-3}. \quad (1)$$

Here J_P^{Max} is the rate at which the pump cycles when $[Na^+]_i$ and $[K^+]_o$ are at saturating levels. K_m^{Na} and K_m^K are the pump's affinities for Na_i^+ and K_o^+, respectively. The parameter α_X is a stoichiometry factor that has to be entered when expressing actual ion flows. We adopt the convention that inward flow carries a + sign and we thus have $\alpha_{Na} = -3$ and $\alpha_K = 2$. The activity of the pump also depends on V_m, but for the range of V_m that we are looking at, its variations are small. So to keep the model simple and to limit the number of adjustable parameters we neglect this dependence. Throughout our experiments the [ATP]/([ADP][P]) ratio is buffered at a saturating level and it therefore does not figure in Eq. (1).

Parameters of the Na,K,2Cl-cotransporter that are useful for our model have not been determined to our knowledge. As the cycle of the Na,K,2Cl-cotransporter does not involve net transport of charge, we
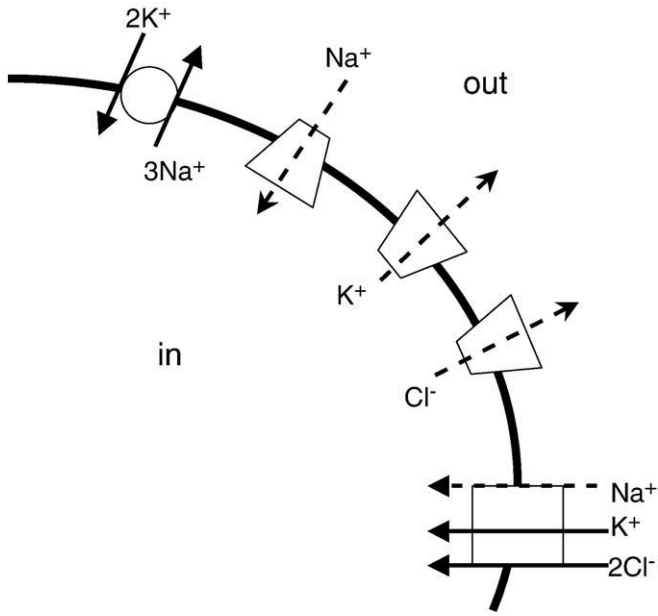
Fig. 1. Overview of the components that make up our model. Solid arrows indicate transport against the electrochemical potential. Dashed arrows indicate transport that follows the electrochemical potential. On the left top is the Na,K-ATPase. This pump utilizes the free energy released by one ATP hydrolysis to import three sodium ions and extrude two potassium ions. The trapezoids denote ion channels that allow for passive ion flux. The arrows indicate the direction of such flux under the steady state conditions that we analyze. The rectangle at the right bottom represents the Na,K,2Cl-cotransporter. In the course of its cycle this symporter allows one sodium ion to move down the electrochemical gradient. A potassium ion and two chloride ions are carried along up their electrochemical gradient.

simply assume that the cycling frequency of the Na,K,2Cl-cotransporter is proportional to the sum of the transmembrane chemical driving forces of the involved ions:

$$
\begin{aligned}
J_{cot}&\left([Na^+]_i, [K^+]_i, [Cl^-]_i\right)\\
&= \beta_X J_{cot}^0 \left[\log\left(\frac{[Na^+]_o}{[Na^+]_i}\right) + \log\left(\frac{[K^+]_o}{[K^+]_i}\right) + 2\log\left(\frac{[Cl^-]_o}{[Cl^-]_i}\right) \right].
\end{aligned} \tag{2}
$$

There is a factor 2 for Cl^- because two chloride ions are imported during a cycle. β_X is again a stoichiometry factor for which we have $\beta_{Na} = 1$, $\beta_K = 1$, and $\beta_{Cl} = 2$. It is because of a lack of information on the Na,K,2Cl-cotransporter and to keep our model as simple as possible that we use this linear, one-parameter dependence on osmolarity [21].

The passive ion fluxes of Na^+, K^+ and, Cl^- through membrane channels depend on electrochemical gradients and permeabilities. Goldman derived an equation for the flux of ion X resulting from the combined effect of a chemical and an electric potential [22]:

$$
J_X(U) = -P_X \frac{U\left([X]_i e^U - [X]_o\right)}{e^U - 1}. \tag{3}
$$

Here $[X]_i$ and $[X]_o$ represent the concentrations of ion X inside and outside the cell, respectively. In our case X stands for Na^+, K^+ or Cl^-. The variable U represents a dedimensionalized electric transmembrane potential: $U = z_j F V_m / RT$, where F is Faraday's constant, V_m is the electric transmembrane potential and z_j is the charge value of the ion ($+1$ for Na^+ and K^+, and -1 for Cl^-). At 35 °C the factor F/RT is 38 V^{-1}. P_X stands for the permeability of the membrane to an ion X. J_X gives the resulting particle flow from the outside to the inside of the cell. Our interest is in the steady states. We therefore do not take

characteristics of the kinetics, i.e., time delayed activation and inactivation of P_{Na} and P_K, into account.

P_{Na} and P_{Cl} are assumed constant in our model. But P_K carries a dependence on V_m and $[K^+]_o$. We will use the following, empirically based, description [13,14,23,24]:

$$
P_K\left(V_m, [K^+]_i, [K^+]_o\right) = P_0 + \frac{\bar{P}_K}{\sqrt{[K^+]_o}}\left(1 + \exp\left[\frac{V_m - V_h}{V_s}\right]\right)^{-1}. \tag{4}
$$

P_0 is a constant that represents the permeability due to K^+ channels other than IRKs. The IRK channels are voltage gated and the term in parentheses establishes a Boltzmann distribution for the open/closed partition. V_s expresses how sensitive the open/closed distribution is to changes in V_m. V_h is the voltage at which the open/closed distribution is fifty–fifty [25]. V_h appears to be close to E_K, the chemical potential of potassium [24]. We thus write $V_h = V_K + \Delta V_h$. The ΔV_h creates a small range in which the IRK is open even though $V_m > E_K$. As was mentioned before, upon decreasing $[K^+]_o$, the switch from the hyperpolarized to the depolarized state occurs when $(V_m - E_K)$ becomes too large. Obviously, a larger ΔV_h will allow us to go to lower values of $[K^+]_o$. From experiment it is apparent that the IRK channels can "sense" the electric membrane potential as well as the intracellular and extracellular potassium concentrations. Eq. (4) describes this sensing. The underlying mechanisms for the sensing are the focus of much research activity [26].

For all of the involved ions the change per unit of time of the intracellular concentration, i.e. $d[X]_i/dt$, can be expressed as the sum of all the fluxes involving that ion multiplied by surface-to-volume ratio of the involved cell:

$$
\frac{d[X]_i}{dt} = \frac{S}{B}(J_X + J_P + J_{cot}). \tag{5}
$$

Here B represents cell volume and S represents cell surface area. Our experiments involve long cylindrical muscle cells with a radius of about 20 μm. This leads to $B/S = 10$ μm. We assume this ratio to be a cell parameter that remains constant throughout the experiment. In [27] methods similar to ours are used, but these authors allow for a variation of the B/S-ratio.

Going from particle fluxes to electrical currents we take a positive current to be one of cations that go from the outside to the inside. So for the change in the transmembrane potential due to the fluxes $d[X]_i/dt$ we have:

$$
\frac{dV_m}{dt} = \frac{FB}{C_m S}\left(\frac{d[Na^+]_i}{dt} + \frac{d[K^+]_i}{dt} - \frac{d[Cl^-]_i}{dt}\right). \tag{6}
$$

Here F is again Faraday's constant and C_m is the specific membrane capacitance. We take $C_m = 8.0 \times 10^{-6} F/cm^2$. It is because of convolutions of the membrane and the presence of the T-tubular system that we take a value of the specific membrane capacitance that is about 8 times larger than that of an ordinary lipid bilayer [13]. We next take $q = FB/C_m S$ and since the specific membrane capacitance does not vary much between cells, q is a constant that effectively only depends on cell geometry. In our computations we use $q = 12,183$ V/M (volts/molar concentration). Essentially, q is a conversion factor that gives the transmembrane voltage that results from the charge of a mole of monovalent ions in the cell. We integrate Eq. (6) with respect to time and express V_m in terms of $[Na^+]_i$, $[K^+]_i$, and $[Cl^-]_i$:

$$
V_m = q\left([Na^+]_i + [K^+]_i - [Cl^-]_i\right) + V_0. \tag{7}
$$

V_0 enters the equation as an integration constant. Physically, V_0 represents the contribution to the transmembrane potential of ions

other than Na^+, K^+, and Cl^-. These include ions like Ca^{2+}, Mg^{2+}, and the, mostly negatively charged, larger organic molecules (ATP, ADP, proteins, sugars, DNA, etc.). Because q and V_0 are so large, submicromolar changes in ionic concentration lead to significant millivolt changes in V_m. For all practical purposes, Eq. (7) imposes the condition that $([Na^+]_i + [K^+]_i - [Cl^-]_i)$ is constant. In our simulation we could have used that constancy as a shortcut in the computations. But we decided to not take such a shortcut and, instead, stay with the full dynamics.

Steady state means that all the time derivatives in the above equations are zero. The resulting algebraic system connects the transmembrane electric potential to ion concentrations and membrane permeabilities. The Goldman–Hodgkin–Katz (GHK) equation is commonly used in electrophysiology and a discussion of this equation is included in many authoritative textbooks [2,25,28]. This equation expresses the membrane potential in terms of membrane permeabilities and ion concentrations. However, it is derived on the basis of the assumption that the net flow of charge through the channels is zero. That assumption does not apply in our model. The Na,K-ATPase is electrogenic, i.e., it generates a net electric current. The cotransporter is electroneutral, so in our model the net flow through the channels should carry a current equal and opposite to the Na,K-ATPase current. There is no "quick fix" of the GHK equation to take care of this effect [27]. Nevertheless, the GHK equation can ultimately help us to obtain an order of magnitude estimate to compare to our model results.

Our expression for the potassium permeability constitutes a serious analytical complication. In our model P_K and V_m depend on each other. It can thus be understood that for the same $[K^+]_o$, a low-P_K depolarized state can coexist with a high-P_K hyperpolarized state [14].

3. Results

In our experiments we measured the transmembrane potential of superficial cells of the lumbrical muscle of the mouse *in vitro*. Cells were impaled with fine tipped glass microelectrodes (filled with 3.0 M KCl and tip resistance >20 MΩ) and ion concentrations in the extracellular medium were under our control. The electrodes remained in the cell for the entire duration of the experiment [14,17,18,21]. We first let the cell come to a steady state with the physiological value $[K^+]_o = 5.7$ mM and we then measure V_m. Our estimate for $[K^+]_o$ may be considered high, but that will not change our eventual results. Even the more recent lower estimates are well outside of the range where we find bistability.

The triangles in Figs. 2 and 3 show the measured V_ms of actual muscle cells as $[K^+]_o$ was decreased in small steps. After each step we give the system sufficient time to reach the new steady state [21]. Generally, at some critical value of $[K^+]_o$, the cell will switch to the depolarized state. We further decrease $[K^+]_o$ to 0.76 mM and then commence a stepwise increase back to 5.7 mM. On the way back to 5.7 mM we indicate the steady state transmembrane potential in Figs. 2 and 3 with circles. In the course of increasing $[K^+]_o$ the switch to the hyperpolarized state occurs at a significantly higher value for $[K^+]_o$ than the value at which, previously, the switch to the depolarized state occurred. The figures thus reveal an obvious hysteresis loop and a distinct region of bistability.

The changes of $[K^+]_o$ were too slow to induce an action potential (which may drive a cell to another steady state). Generally, relaxation to a new steady state value of V_m after changing $[K^+]_o$ was a matter of minutes. When it was obvious that a switch to the other branch of solutions was occurring, we waited for about half an hour. More details on the materials and methods are presented in past publications of our group [14,17,18,21].

We next performed the same loop on the same cell in an altered medium. For Fig. 2 this was a medium with 75 μM bumetanide. For Fig. 3 it was a medium that we had made hyperosmotic through the addition of the membrane impermeable polyethylene glycol 300.
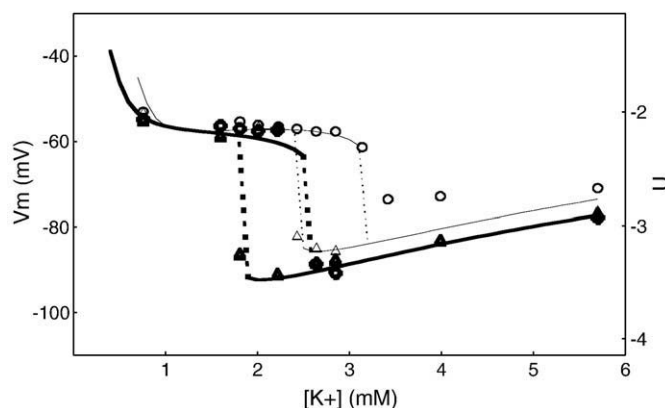

Fig. 2. Recorded hysteresis loops of one and the same cell with bumetanide (thick symbols and curves) and without bumetanide (thin symbols and curves) in the medium. Experimental data also appeared in [19]. Triangles indicate the transmembrane voltage as $[K^+]_o$ is decreased from 5.7 mM to 0.76 mM. Circles show the transmembrane voltage as $[K^+]_o$ is increased again. After a change in $[K^+]_o$, it took the cell about 4 min to reach a new steady state. The transitions from the hyperpolarized branch to the depolarized branch and vice versa (dashed lines) took about 30 to 45 min. The curves indicate model fits. The parameter values of these fits are given in Table 1. Bumetanide removes chloride as an influence on the membrane potential and is here observed to shift the bistable region to lower values of $[K^+]_o$.

Running the two loops, the control loop and the subsequent loop with the altered medium, takes about 4 h. Deterioration of the cell in such a period of time occurs, but is generally small. Each of the two kinds of two-loop experiments was done three times. Outcomes were found to be similar and figures show representative results. For the control loop the bistable region was found to be between 1.57 mM (± 0.09 mM, $n = 13$) and 2.77 mM (± 0.12 mM, $n = 13$). For the loops with bumetanide in the medium the bistable region was found to be between 1.25 mM (± 0.16 mM, $n = 3$) and 2.36 mM (± 0.16 mM, $n = 3$). For the loops with a hypertonic medium the bistable region was found to be between 2.33 mM (± 0.31 mM, $n = 2$) and 3.14 mM (± 0.29 mM, $n = 2$). Some of the results of these experiments are also found in [19]. In the experiments where we ran a control loop and a bumetanide loop or hypertonic loop on one and the same cell we can also express the bumetanide and hypertonic results as percentages of the control. We then exclude the variation between cells. Doing this one finds that with bumetanide the switches are at potassium concentrations that are $67 \pm 4\%$ and $83 \pm 8\%$ for respectively the switch to the depolarization branch and the switch to the repolarization branch. In the hypertonic situation these values are $181 \pm 9\%$ and $136 \pm 6\%$.

For our model calculations we take the following approach. With the measured value of V_m and the extracellular concentrations at the beginning of each experiment, we go to Eq. (5) and obtain the intracellular concentrations by setting $d[Na^+]_i/dt = 0$, $d[K^+]_i/dt = 0$, and $d[Cl^-]_i/dt = 0$ and then solving the algebra. Substituting the obtained values $[Na^+]_i$, $[K^+]_i$, and $[Cl^-]_i$ into Eq. (7) then leads to the value for V_0. For a given cell, the value for V_0 so calculated at the physiological starting point will be kept the same throughout further calculations. Independent estimates for the values of many of the involved parameters (J_P^{Max}, P_{Na}, P_m^K, P_m^{Na}, etc.) can be found in the literature.

To check the model against the experiments, we change the value $[K^+]_o$ from the aforementioned 5.7 mM and we compute for which values of $[Na^+]_i$, $[K^+]_i$, and $[Cl^-]_i$ a steady state (i.e. $d[X_i]/dt = 0$ in Eq. (5)) occurs. It is from Eq. (7) that we then infer V_m. It turns out that the ultimate V_m is orders of magnitude smaller than $q[Na^+]_i$, $q[K^+]_i$, $q[Cl^-]_i$, and V_0 themselves. $[Na^+]_i$, $[K^+]_i$, and $[Cl^-]_i$ are all of more than mM magnitude, but the ultimate V_m is brought about by a μM imbalance between positive and negative ions. This leads to complications in the computation of the steady state. A simple
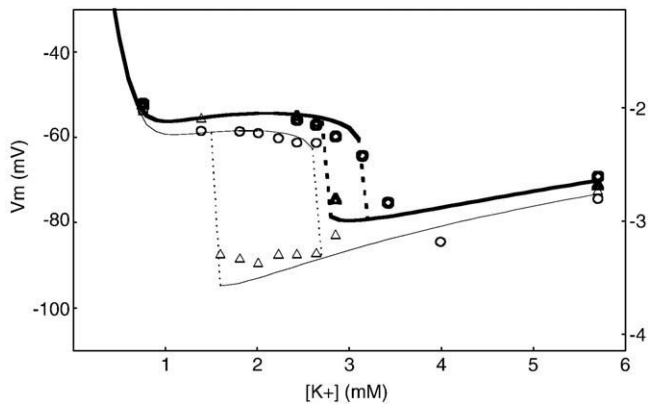
Fig. 3. Recorded hysteresis loops of one and the same cell in a normal (289 mosmol/kg) medium (thin symbols and curves) and in a hyperosmotic (344 mosmol/kg) medium (thick symbols and curves). Experimental data also appeared in [19]. Triangles indicate the transmembrane voltage as $[K^+]_o$ is decreased from 5.7 mM to 0.76 mM. Circles give the transmembrane voltage as $[K^+]_o$ is increased again. After a change in $[K^+]_o$, it took the cell about 4 min to reach a new steady state. The transitions from the hyperpolarized branch to the depolarized branch and vice versa (dashed lines) took about 30 to 45 min. The curves indicate model fits. The parameter values of these fits are given in Table 1. Hyperosmolarity increases the turnover rate of the Na,K,2Cl-cotransporter and thus drives the chloride electrochemical potential further away from zero. The figure shows how the augmented chloride contribution to the membrane potential drives the bistability to higher values of $[K^+]_o$.

Newton scheme often appeared to not converge to a steady state. Using *Mathematica* [29] we found it actually easier to simulate Eq. (5) as a system of differential equations. We could then see how $[Na^+]_i$, $[K^+]_i$,

and $[Cl^-]_i$ converge in real time to new stable steady state values after every change of $[K^+]_o$. Following this approach we actually simulated what was happening in real time after the stepwise change of $[K^+]_o$ was performed in the experiments. The curves in Figs. 2 and 3 show the results of the model simulation. The parameters that produce the fits are compiled in Table 1.

As was mentioned before, estimates for many of the relevant parameter values can be taken from the literature. A number of input parameters was specified before the calculations started. After determining V_0, we checked whether the concentrations $[Na^+]_i$, $[K^+]_i$, and $[Cl^-]_i$ were in the expected range (see Introduction). We also checked $([Na^+]_i + [K^+]_i + [Cl^-]_i)$ and ensured that the total osmotic content of the cell did not vary too much. We never observed any volume changes in the course of our experiments and conclude that a cell can respond adequately to hypertonicity by increasing its own osmotic value. The values of the sum $([Na^+]_i + [K^+]_i + [Cl^-]_i)$ at the resting potential are also listed in Table 1. The results of our eventual fits, depicted in Figs. 2 and 3, are largely consistent with what has been found with other methods (see Discussion).

In fitting the model curves to the experimental data, a few aspects become obvious and are worth pointing out. On the depolarized branch, when the IRK channels are closed, it is the ratio P_{Na}/P_0 that largely determines V_m. The value $\bar{P}_K$ (cf. Eq. (4)) establishes the level of hyperpolarization when the IRKs are open. The two most important values for the position of the bistable region are the parameters ΔV_h and V_s that underlie the opening and closing of the IRK channels (cf. Eq. (4)). The sensitivity constant V_s is seen to determine the horizontal width of the bistable region in the V_m vs. $[K^+]_o$ graph. The parameter ΔV_h, which describes the deviation of V_h from E_K is what determines where along the $[K^+]_o$-axis the bistable region is centered.

Table 1
A list of parameter values to fit the experimental data depicted in Figs. 2 and 3.

Parameter	Bumetenide		Hypertonicity		Dimensions	Condition
	Control	Experimental	Control	Experimental		
P_{Cl}	1.90E−05	1.90E−05	1.90E−05	1.90E−05	cm/s	Derived in Appendix A
P_0	6.06E−07	6.06E−07	6.08E−07	6.08E−07	cm/s	Adjusted to obtain the correct ratio P_{Cl}/P_K
P_{Na}/P_0	0.08	0.154	0.075	0.08	–	Adjusted to fit depolarized V_m at low $[K^+]_o$
P_K/P_0	0.65	0.55	0.45	0.7	–	Adjusted with P_0 to fit hyperpolarized V_m
V_m	−73.55	−77.35	−73.30	−70.15	mV	Taken as the average of the measured values
V_s	8.9	7.5	8.0	10.5	mV	Determines the range of the hyteresis loop
ΔV_h	11.8	19.3	18.8	10.7	mV	Determines switch-off in the depolarized curve (These two parameters are mutually interactive)
J_p^{max}	5.50E−11	4.50E−11	5.50E−11	3.80E−11	mol/cm^2 s	Determines the strength of the pump
K_m^K	1.30	0.50	1.20	0.82	mM	Kinetic constant for K^+ in pump: determines the low $[K^+]_o$ behavior
K_m^{Na}	7.00	7.00	6.00	6.00	mM	Kinetic constant for Na^+ in pump: partially determines $[Na^+]_i$
Osm	0.296	0.296	0.296	0.344	Osm	Measured osmolality of external medium
Osm_0	0.268	0.268	0.268	0.268	Osm	Measured osmolality when flux of cotransporter is zero
OsmSense	2.40E−09	0.00E+00	2.40E−09	1.40E−09	mol/cm^2 s	Determines the strength of the cotransporter
J_{cot}^0	6.72E−11	0.00E+00	6.72E−11	1.064E−10	mol/cm^2 s	Activity of the cotransporter: $(Osm − Osm_0)*OsmSense$
Output parameters						
V_0	−1718.54	−1871.33	−1664.85	−1699.58	V	Integration constant for V_m
P_{Cl}/P_K	5.66	4.53	5.82	6.29	–	Should be ≳3
P_K/P_{Na}	69.20	44.91	71.54	62.13	–	Should be in the range 50 to 100
$[Na^+]_i$	12.68	17.04	10.11	14.94	mM	In control $[Na^+]_i$ should be approximately 14 mM
$[K^+]_i$	136.84	143.61	135.08	134.26	mM	In control $[K^+]_i$ should be approximately 140 mM
$[Cl^-]_i$	8.47	7.06	8.54	9.71	mM	In control $[Cl^-]_i$ should be approximately 8 mM
$[Cl^-]_{i,Eq}$	8.15	7.06	8.22	9.26	mM	Equilibrium $[Cl^-]_i$ at V_m
$[Cl^-]_i − [Cl^-]_{i,Eq}$	0.32	0.00	0.32	0.45	mM	Cl^- accumulation compares well with experimental values
$[Na^+]_i + [K^+]_i + [Cl^-]_i$	158.0	167.7	153.7	158.9	mM	Total osmolarity of permeable ions inside the cell
$J_{cot}/\beta\chi$	−8.99E−12	0	−8.79E−12	−1.21E−11	mol/cm^2 s	Gives an estimate to the rate of the cotransporter
$J_P/\alpha\chi$	−9.75E−12	−1.35E−11	−9.28E−12	−1.05E−11	mol/cm^2 s	Gives an estimate to the rate of the pump

Input parameters were measured in experiment or taken from the literature. Output parameters were obtained by matching the model with experimental outcomes as shown in Figs. 2 and 3. The given values are for $[K^+]_o = 5.7$ mM. How P_{Cl} is initially estimated is shown in the Appendix A. The curves in Figs. 2 and 3 can be shifted by changing permeability ratios and other parameters. We adjusted P_0 to get a P_{Cl}/P_K slightly larger than 3 (given in [4]). On the depolarized branch, when IRKs are closed, P_{Na}/P_0 determines V_m and was appropriately set. P_K/P_0 was likewise set in agreement with the hyperpolarized V_m. Our value for P_K leads to $\bar{P}_K / \left(P_0 \sqrt{[K^+]_o} \right) \approx 10$ at physiological conditions. V_m is the average of before and after the entire experiment of Figs. 2 and 3. The parameter J_{cot}^0 is found to depend on the osmolarity ("Osm") of the medium. Following [21], we assume a linear dependence $J_{cot}^0 = OsmSense(Osm − Osm_0)$, where "OsmSense" fixes the sensitivity of J_{cot}^0 to osmolarity and "Osm_0" is the osmolarity at which the cotransporter comes to a standstill. The obtained values for the intracellular concentrations are very reasonable. The estimates for the chloride accumulation and for the cotransporter flow constitute a main result of this work (see text).

It is the Na^+ potential that drives the Na,K,2Cl-cotransporter. So, ultimately, the cotransporter's energy supply derives from the ATP driven Na,K-pump. Obviously, the cotransporter's Cl^--transport against the net electrochemical Cl^--potential indirectly presents another load on the Na,K-pump. Going back to the explanation that was given at the end of the Introduction (third paragraph from the end), we can then understand that, with more chloride transport, the system will make an earlier switch to the depolarized branch when $[K^+]_o$ is decreased. So we get a switch at higher $[K^+]_o$ when the cotransporter is stimulated with a hyperosmotic medium. The presence of bumetanide, on the other hand, eliminates chloride traffic and should push the bistable region to smaller values of $[K^+]_o$. Experiments affirm these expectations and the model gives a good accounting (cf. Figs. 2 and 3).

In Fig. 2 we see that, for the physiological condition and on the remainder of the hyperpolarized branch, there is a further hyperpolarization of about 3 mV after the addition of bumetanide to the medium. At the end of Section 2 we mentioned how the GHK equation can provide an approximation. In terms of the GHK equation, addition of bumetanide brings us from

$$V_m = \frac{RT}{F}\log\left[\frac{P_K[K^+]_o + P_{Na}[Na^+]_o + P_{Cl}[Cl^-]_i}{P_K[K^+]_i + P_{Na}[Na^+]_i + P_{Cl}[Cl^-]_o}\right] \tag{8}$$

to

$$V_m = \frac{RT}{F}\log\left[\frac{P_K[K^+]_o + P_{Na}[Na^+]_o}{P_K[K^+]_i + P_{Na}[Na^+]_i}\right]. \tag{9}$$

At our close to physiological starting point, i.e. $[K^+]_o = 5.7$ mM, $[Na^+]_o = 148$ mM, and $[Cl^-]_o = 130$ mM, we measured $V_m = -73$ mV before and $V_m = -76$ mV after the addition of bumetanide. Taking $[K^+]_i = 132$ mM, $[Na^+]_i = 10$ mM, and $P_{Cl} = 3P_K$ [4,30,31] we find with these equations that $[Cl^-]_i$ exceeds $[Cl^-]_i^{eq}$ (which is to be calculated from $V_m = (RT/F)\log([Cl^-]_i^{eq}/[Cl^-]_o)$ at $V_m = -73$ mV) by about 0.36 mM. This estimate, however, assumes that $[Na^+]_i$ and $[K^+]_i$ do not change upon the addition of bumetanide and it is bound to be inaccurate. It is inaccurate because Na,K-ATPase and the Na,K,2Cl-cotransporter couple the flows of the involved ions. Therefore $[Na^+]_i$ and $[K^+]_i$ change to new steady state values after the addition of bumetanide. Our full model does take such changes into account and leads to an estimate of 0.31 mM for the accumulation of chloride above the equilibrium concentration. For the hyperosmotic medium the GHK Eqs. (8) and (9), lead to $([Cl^-]_i - [Cl^-]_i^{eq}) = 1.4$ mM. Our model predicts to 0.45 mM for this case.

4. Discussion

As was mentioned before, the Na,K,2Cl-cotransporter accumulates chloride in the cell to slightly above the concentration that would occur if the intracellular and extracellular chloride were at electrochemical equilibrium. It is obvious that there is a connection between this accumulation and the quantities J_{cot} for the cotransporter driven inflow and P_{Cl} for the chloride permeability of the membrane. A larger P_{Cl} leads to "easier" outflow and, thereby, to a smaller necessary accumulation to compensate for the inflow. Estimates of the involved quantities and parameters have varied. Direct measurement in mammalian skeletal muscle of the chloride accumulation with chloride sensitive electrodes led to $1.4 (\pm 1.2)$ mM [31]. With similar methods, others [32,33] have found values at the low end of this order of magnitude estimate. It is apparent that the chloride accumulation above the electrochemical equilibrium concentration is too small to be meaningfully established with chloride sensitive electrodes. To obtain that accumulation two measured quantities that are almost equal have to be subtracted and the resulting difference comes with a relative error that is much larger than the relative error of the original measured quantities. It has been suggested that chloride permeability can increase with osmotic stress [34]. But in our model P_{Cl} is constant and P_K is adjusted such that the ratio P_{Cl}/P_K is about 5 [4]. For the potassium permeability we find, in turn, that it is about ten times as large as the sodium permeability. In physiological conditions we, furthermore, infer from the values of $\bar{P}_K$ and P_0 that the IRKs account for about 85% of the potassium permeability.

Ba^{2+} blocks the IRKs and upon its application the membrane potential relaxes to a new steady state. In Ref. [17] such relaxation was employed to come to an estimate of J_{cot}. This relaxation, which takes about 1 to 4 min, was recorded with and without bumetanide in the medium and fitted with a single exponential. J_{cot} was thus found to be 1.4×10^{-12} mol cm^{-2} s^{-1}, i.e. about an order of magnitude smaller than our estimate (see Table 1). However, the starting point for the J_{cot}-estimate of Ref. [17] was the aforementioned approximate 1.4 mM chloride accumulation of Ref. [31]. Ref. [17], furthermore, used the formula $V_m = (RT/F)\log([Cl^-]_i/[Cl^-]_o)$ to relate a change in transmembrane voltage after the addition of bumetanide to a change in $[Cl^-]_i$. Such a correspondence between cotransporter-caused chloride accumulation and membrane potential can, at best, be very approximate, as the Na,K,2Cl-cotransporter also moves sodium and potassium across the membrane. Moreover, the intracellular concentrations of the three involved ions are all coupled to each other and to the membrane potential. Our model incorporates these couplings. The full effect of the addition of bumetanide can only be assessed through a numerical simulation like ours.

The Na,K,2Cl-cotransporter is a carrier. As such, it ought to exhibit Michaelis–Menten type saturation with increasing concentrations of the carried ions. It is because of a lack of available data on the cotransporter that we opted for the simple one-parameter description of the cotransporter's turnover. Neglecting the saturation may be particularly inappropriate in the hyperosmotic situation [19]. A more accurate model can be constructed as more data on the cotransporter will become available.

We did not perform a systematic general and exhaustive search over the entire parameter space to find what values lead to the best fit. There are too many parameters for such an approach to lead to a unique result. Moreover, such an approach would not be sensible as the model is approximate to begin with. We started with values that were close to existing estimates and kept the values in an acceptable range as we perfected the fits. Our goal was for our simulation to merely reproduce the experimental phenomena (the bistability foremost) with known facts, estimates, and relationships.

The Na,K-ATPase has been well researched and the parameter values that we report in Table 1 are in the established range. K_m^K and K_m^{Na} are used as described in Eq. (1). Customarily, the K_m^X is defined as the concentration at which the pump operates at half the speed of what it would be at saturating $[X]$. Because of the powers -2 and -3 in our description of the Na,K-ATPase (cf. Eq. (1)), our case is slightly different. We have 1/8 of the saturated turnover at $[Na^+]_i = K_m^{Na}$ and 1/4 of the saturated turnover at $[K^+]_o = K_m^K$. The authoritative textbook by Läuger [2] gives $K_m^{Na} = 0.6$ mM and $K_m^K = 0.2$ mM for the values at which the pump operates at the half maximal rate. However, estimates for these parameters have varied widely. The more recent Ref. [35] reports $K_m^K = 0.8$–1.5 mM and $K_m^{Na} \sim 15$ mM. These numbers appear closer to our estimates.

J_P^{Max} is not just a molecular property. J_P^{Max} is also proportional to the number of pumps per unit area on the cell membrane. J_P^{Max} can thus vary widely from cell to cell. Reference [36] lists the estimated maximal transmembrane flux of sodium ions for three different mammalian muscle cells. These estimates vary from 25 to 83 pmol s^{-1}cm^{-2}. The associated J_P^{Max} is found after dividing these numbers by three. Our numbers in Table 1 appear about an order of magnitude higher than these estimates. Likewise, P_{Na} depends linearly on the permeability of a channel as well as on the number of channels per unit area of cell

membrane. The values in Table 1 appear close to the $P_{Na} = 5.37$ $(\pm 0.30) \times 10^{-8}$ cm s^{-1} that is reported in Ref. [37] for *Xenopus laevis* oocytes.

The table shows how the cotransporter actually cycles about as much as the Na,K-ATPase. From the numbers in the table it can be inferred that the inward sodium flow through the cotransporter has roughly 30% of the magnitude of the outward sodium flow through the Na,K-ATPase. For potassium, cotransporter flow is about 50% of the flow through the Na,K-ATPase. At steady state it thus appears to not be legitimate to treat cotransporter activity as a mere perturbation on the dynamics of a system with only Na,K-ATPase and channels for sodium and potassium.

The parameter V_s quantifies the sensitivity of the IRK's open-closed ratio to the membrane potential. Over the course of more than three decades the inward rectification has been fitted many times to a Boltzmann distribution. Estimates for V_s have consistently fallen in the range between 7 mV and 15 mV [38]. We account for the change of the width and location of the bistable region in Figs. 2 and 3 primarily with changes in the IRK parameters V_s and ΔV_h. This may seem puzzling. After all, one is tempted to think that V_s and ΔV_h are consequences of the internal structure of the IRK channel and one would not expect V_s and ΔV_h to depend on ion concentrations. However, it has been reported that other ions (like Mg^{2+}) are involved in the closing of the IRKs and that concentration levels of intracellular polyamines can modulate properties of the IRK channel [3,39]. It is possible that Mg^{2+} and polyamine concentrations are behind the variation in V_s and ΔV_h that we see in Table 1. The variation of V_s that we see is within the aforementioned 7 to 15 mV range. For ΔV_h we have not found any estimates in the literature.

Appendix A

In order to relate the model calculations to measured data, we need estimates for the membrane permeability for chloride, P_{Cl}, and for the cotransporter flow, J_{cot}. For that purpose we use experimental data presented in Ref. [17]. In that reference the same preparations as here were used.

In Ref. [17] it is described how Ba^{2+} was added to the extracellular medium. Barium rapidly blocks the inwardly rectifying potassium channel (called here IRK). An exponential relaxation of a few minutes to a new membrane potential occurs after such blocking. How the values of P_{Cl} and J_{cot} can be derived from the comparison of the relaxation time without (the control) and with bumetanide (that blocks the cotransporter) in the medium will be shown in this Appendix. In Ref. [17] the imprecise chloride accumulation estimate $(1.4 \pm 1.2$ mM$)$ of Ref. [31] was utilized to achieve an estimate of J_{cot}. Our approach also relies on estimations by others; in particular estimations for the permeability ratios for potassium, sodium and chloride and for the concentrations of these ions in the cell under physiological conditions. However, these values are more precisely known.

After the blocking of the IRKs by Ba^{2+}, the system relaxes to a new steady state. As P_{Cl} is much larger than P_K and P_{Na}, the relaxation to a new steady state value of V_m is primarily associated with the influx of chloride into the cell. The difference of the relaxation times with and without bumetanide can provide the value of the cotransporter flow J_{cot}.

With bumetanide in the medium, the accumulation of chloride is negligible and we have $V_m = E_{Cl}$ in steady state. This allows us to leave out the chloride contribution in the GHK-equation as in Eq. (9). In this case we measure $V_m = -76$ mV before the addition of Ba^{2+}. We make the Mullins and Noda correction for the rheogenic properties (see Chapter 4 of Ref. [2]) of the Na/K-pump and we find that such V_m is well fitted with physiological values $[K^+]_i = 132$ mM, $[Na^+]_i = 10$ mM, and $P_K/P_{Na} = 78$. With bumetanide and Ba^{2+} in the medium, we measure $V_m = -51$ mV after full relaxation. With the same values for $[K^+]_{mi}$ and $[Na^+]_i$ we then find $P_K/P_{Na} = 11$. A more detailed

adjustment of the concentrations of sodium and potassium produces only a minor change in P_K/P_{Na}.

The driving force behind the chloride inflow is the difference between the actual membrane potential and the equilibrium potential for chloride, i.e. $V_m - E_{Cl}$, where $E_{Cl} = (RT/F)\log([Cl^-]_i / [Cl^-]_o)$. When V_m is reduced upon the addition of Ba^{2+}, we get $V_m > E_{Cl}$ and chloride flows into the cell. We can describe the relaxation as follows:

$$[Cl^-]_i(t) = \left(\frac{E_{Cl}(0)}{V_m(0)}\right)[Cl^-]_o exp[-u(t)],$$

where u is a dedimensionalized representation of V_m (see Introduction of the main text). The slope of $[Cl^-]_i(t)$ at $t = 0$ (i.e. directly after the addition of Ba^{2+}) can be approximated by differentiating this expression with respect to time and setting $t = 0$:

$$\frac{d}{dt}[Cl^-]_i(t = 0) \approx \left(\frac{E_{Cl}(0)}{V_m(0)}\right)[Cl^-]_o \frac{\Delta u}{\tau} \exp[-u(0)].$$

Here Δu is the dedimensionalized total change in V_m in the course of the entire relaxation and τ is the characteristic relaxation time that results when the relaxation of the membrane potential is fitted with a single exponential. All the values on the right hand side of this equation can be measured or well approximated. As in Eq. (5), we then obtain an estimate for the flux through the cotransporter

$$J_{Cl}(t = 0) = \frac{1}{4}d\left(\frac{d[Cl^-]_i(t)}{dt}\right)_{t=0},$$

where d denotes the diameter of the cylindrical muscle cell. For the cases with and without bumetanide the difference of the J_{Cl}s is due to the constant cotransporter flux J_{cot}. Without bumetanide the relaxation time τ is measured as 127 ± 7 s and with bumetanide that relaxation time is measured to be 182 ± 23 s [17]. This leads to $J_{cot} = 20 \pm 8$ pmol cm^{-2} s^{-1}.

In the main text we also examine the situation with a hypertonic medium. Hypertonicity increases the flow through the cotransporter. The above analysis is readily repeated for the hypertonic situation and is found to lead to $J_{cot}^{hyp} = 28 \pm 16$ pmol cm^{-2} s^{-1}.

In the control situation, without bumetanide, the steady state transmembrane potential before the addition of barium is -73 mV. A small hyperpolarization to -76 mV occurs when just bumetanide is added. Such 3 mV hyperpolarization is associated with intracellular chloride decrease, i.e. an intracellular chloride concentration that is slightly higher in the control situation than what it would be at the chloride equilibrium that we have with bumetanide. Ref. [4] reports a P_{Cl}/P_{rmK} that is at least 3. A larger value of P_{Cl}/P_K would make the chloride decrease smaller. This is because the passive efflux of chloride, being equal to the influx through the cotransporter, needs a smaller driving force when the value of P_{Cl} is larger. In the control steady state J_{cot} is equal and opposite to the passive outward flow through the chloride channels. With Eq. (3) of the main text we next infer $P_{Cl} = (21 \pm 2) \times 10^{-9}$ cm s^{-1} in control and $P_{Cl} = (15 \pm 2) \times 10^{-9}$ cm s^{-1} in the hypertonic medium. These values are consistent with the range we assumed them to be in at the beginning of the derivation.

References

[1] J.G. Nichols, A.R. Martin, B.G. Wallace, From Neuron to Brain, Sinauer Associates Inc., Sunderland, MA, 1992.
[2] P. Läuger, Electrogenic Ion Pumps, Sinauer Associates Inc., Sunderland, MA, 1991.
[3] Z. Lu, Mechanism of rectification in inward-rectifier K$^+$ channels, Annu. Rev. Physiol. 66 (2004) 103–129.
[4] A.H. Bretag, Muscle chloride channels, Physiol. Rev. 67 (1987) 618–724.
[5] M. Haas, B. Forbush, The Na–K–Cl cotransporter of secretory epithelia, Annu. Rev. Physiol. 62 (2000) 515–534.
[6] J.M. Russell, Sodium–potassium–chloride cotransport, Physiol. Rev. 80 (2000) 211–276.
[7] K. Strange, Cellular volume homeostasis, Adv. Physiol. Educ. 28 (2004) 155–159.

[8] D.H. Ellison, Diuretic therapy and resistance in congestive heart failure, Cardiology 96 (2001) 132–143.

[9] D. Landau, Potassium-related inherited tubulopathies, Cell. Mol. Life Sci. 62 (2006) 1962–1968.

[10] A.V. Alfonzo, C. Isles, C. Geddes, C. Deighan, Potassium disorders—clinical spectrum and emergency management, Resuscitation 70 (2006) 10–25.

[11] K. Jurkat-Rott, F. Lehmann-Horn, Paroxysmal muscle weakness — the familial periodic paralyses, J. Neurol. 253 (2006) 1391–1398.

[12] A.F. Struyk, S.C. Cannon, Paradoxical depolarization of Ba^{2+}-treated muscle exposed to low extracellular K^+: insights into resting potential abnormalities in hypokalemic paralysis, Muscle Nerve 37 (2008) 326–337.

[13] J. Siegenbeek van Heukelom, The role of the potassium inward rectifier in defining cell membrane potentials in low potassium media, analyzed by computer simulation, Biophys. Chem. 50 (1994) 345–360.

[14] H. van Mil, J. Siegenbeek van Heukelom, M. Bier, A bistable membrane potential at low extracellular potassium concentration, Biophys. Chem. 106 (2003) 15–21.

[15] R.J. Geukes Foppen, J. Siegenbeek van Heukelom, Isoprenaline-stimulated differential adrenergic response of K^+ channels in skeletal muscle under hypokalaemic conditions, Pflugers Arch. 446 (2003) 239–247.

[16] R.J. Geukes Foppen, H.G.J. van Mil, J. Siegenbeek van Heukelom, Osmolality influences bistability of membrane potential under hypokalemic conditions in mouse skeletal muscle: an experimental and theoretical study, Comp. Biochem. Physiol. Part A 130 (2001) 533–538.

[17] R.J. Geukes Foppen, In skeletal muscle the relaxation of the resting membrane potential induced by K^+ permeability changes depends on Cl^- transport, Pflugers Arch. — Eur. J. Physiol. 447 (2004) 416–425.

[18] J. Siegenbeek van Heukelom, Role of the anomalous rectifier in determining membrane potentials of mouse muscle fibres at low extracellular K^+, J. Physiol. 434 (1991) 549–560.

[19] R.J. Geukes Foppen, H.G.J. van Mil, J. Siegenbeek van Heukelom, Effects of chloride transport on bistable behaviour of the membrane potential in mouse skeletal muscle, J. Physiol. 542 (2002) 181–191.

[20] J. Siegenbeek van Heukelom, H.G.J. van Mil, R.J. Geukes Foppen, in: H.V. Westerhoff, et al., (Eds.), BioThermoKinetics of the Living Cell, BioThermoKinetics Press, Amsterdam, 1996, p. 112.

[21] H.G.J. van Mil, R.J. Geukes Foppen, J. Siegenbeek van Heukelom, The influence of bumetanide on the membrane potential of mouse skeletal muscle cells in isotonic and hypertonic media, Br. J. Pharmacol. 120 (1997) 39–44.

[22] H.G. Ferreira, M.W. Marshall, The Biophysical Basis of Excitability, Cambridge University Press, Cambridge, Great Britain, 1985.

[23] S. Hagiwara, K. Takahashi, The anomalous rectification and cation selectivity of the membrane of a starfish egg cell, J. Membr. Biol. 18 (1) (1974) 61–80.

[24] N.B. Standen, P.R. Stanfield, Inward rectification in skeletal muscle; a blocking particle model, Pflugers Arch. 378 (1978) 173–176.

[25] B. Hille, Ionic Channels of Excitable Membranes, Sinauer Associates Inc., Sunderland, MA, 1992.

[26] M. Spassova, Z. Lu, Coupled ion movement underlies rectification in an inward-rectifier $K+$ channel, J. Gen. Physiol. 112 (1998) 211–221.

[27] J.A. Fraser, C.L. Huang, A quantitative analysis of cell volume and resting potential determination and regulation in excitable cells, J. Physiol. (Lond.) 559 (2004) 459–478.

[28] J. Keener, J. Sneyd, Mathematical Physiology, Springer Verlag, New York, 1998.

[29] Wolfram Research, Inc., Mathematica, Version 5.2 (Champaign, IL, 2005).

[30] C.C. Aickin, in: A.F. Alvarez-Leefmans, J.M. Russell (Eds.), Chloride Channels and Carriers in Nerve, Muscle, and Glial Cells, Plenum Press, London, 1990, p. 209.

[31] C.C. Aickin, W.J. Betz, G.L. Harris, Intracellular chloride and the mechanism for its accumulation in rat lumbrical muscle, J. Physiol. 411 (1989) 437–455.

[32] P.J. Donaldson, J.P. Leader, Intracellular ionic activities in the EDL muscle of the mouse, Pflugers Arch. 400 (2) (1984) 166–170.

[33] D. McCaig, J.P. Leader, Intracellular chloride activity in the extensor digitorum longus (EDL) muscle of the rat, J. Membr. Biol. 81 (1) (1984) 9–17.

[34] S. Yamamoto, K. Ishihara, T. Ehara, T. Shioya, Cell-volume regulation by swelling-activated chloride current in guinea-pig ventricular myocytes, Jpn. J. Physiol. 54 (2004) 31–38.

[35] O.M. Sejersted, G. Sjøgaard, Dynamics and consequences of potassium shifts in skeletal muscle and heart during exercise, Physiol. Rev. 80 (2000) 1411–1481.

[36] O.M. Sejersted, in: J.C. Skou, et al., (Eds.), The Na^+,K^+-pump. Part B: Cellular Aspects, Progress in Clinical and Biological Research, vol. 268B, Wiley - Liss, New York, 1988, p. 195.

[37] P.F. Costa, M.G. Emilio, P.L. Fernandes, H.G. Ferreira, K.G. Ferreira, Determination of ionic permeability coefficients of the plasma membrane of *Xenopus laevis* oocytes under voltage clamp, J. Physiol. 413 (1989) 199–211.

[38] R. Wessel, W.B. Kristan, D. Kleinfeld, Supralinear summation of synaptic inputs by an invertebrate neuron: dendritic gain is mediated by an "inward rectifier" K^+ current, J. Neurosci. 19 (14) (1999) 5875–5888.

[39] D.-H. Yan, K. Ishihara, Different polyamine concentrations underlie the regional difference in the strong inward rectifier K^+ current in the heart, Physiol. News 60 (2005) 26–27.